

Cite this article as: Meng Qingyu, You Junhua, Zhou Jifeng, et al. Review on Chemical Synthesis of Nd-Fe-B Magnetic Nanoparticles: Microstructure and Magnetic Properties[J]. Rare Metal Materials and Engineering, 2022, 51(04): 1253-1262.

REVIEW

# Review on Chemical Synthesis of Nd-Fe-B Magnetic Nanoparticles: Microstructure and Magnetic Properties

Meng Qingyu, You Junhua, Zhou Jifeng, Liu Ziyu

School of Materials Science and Engineering, Shenyang University of Technology, Shenyang 110870, China

**Abstract:** High-performance Nd-Fe-B magnets are widely needed in various fields. The purpose of studying Nd-Fe-B nanometer magnetic powder is that the coercivity of the powdered magnets is the largest at the single domain size. The preparation of nanoparticles by the chemical method can better control the microstructure and grain size. Moreover, metal salts as precursors and simplified process routes can significantly reduce costs and energy consumption. In this review, several popular chemical methods for synthesizing Nd-Fe-B nanoparticles were reported, including sol-gel, auto-combustion, microwave-assisted combustion, thermal decomposition, and mechanochemical method. The preparation process and reaction mechanism of these methods were discussed. Finally, the relationship between microstructure and magnetic properties of Nd-Fe-B nanoparticles prepared by different chemical methods was summarized and some future trends and perspectives in the magnetic research areas were submitted.

**Key words:** Nd-Fe-B; magnetic nanoparticles; chemical synthesis; Curie temperature

Magnetic material is an old and widely used functional material. The research and optimization of  $\text{Nd}_2\text{Fe}_{14}\text{B}$  permanent magnetic materials is the further development of magnetic materials, and it is gradually developed to nanometer magnetic materials<sup>[1-5]</sup>. In recent years,  $\text{Nd}_2\text{Fe}_{14}\text{B}$  magnets are widely used in the field of permanent magnetic materials due to the combination of high coercivity ( $H_c$ ) and energy product  $(BH)_{\max}$ , such as electric motors, wind turbines, generators and other novel industries<sup>[6,7]</sup>.

The purpose of the research of nano-scale hard magnetic materials originated from the discovery of the influence of the grain size of magnetic powder on the coercivity in the 1950s<sup>[8,9]</sup>. The study found that the coercivity of powder magnet increases with the reduction of particle size until reaching a maximum at the single domain size, then decreases again for ultrafine particles due to thermal effects, and becomes zero at the superparamagnetic particle size. The first studies on nanoscale magnetic systems were made on amorphous  $R\text{-Fe}$  ( $R=\text{Tb}, \text{Sm}$ ) alloys<sup>[10]</sup>. Since  $R$  is a kind of light rare earth, the  $R\text{-Fe}$  binary alloy has a lower Curie temperature. At the Magnetic and Magnetic Materials

Conference held in Pittsburgh in 1983, two methods for synthesizing iron-based rare earth hard magnets were proposed to solve this problem<sup>[11-15]</sup>. One method involved rapid solidification of the alloy using melt spinning, and the other method was traditional powder metallurgy technology. In 1984, Croat et al<sup>[16]</sup> reported energy products as large as  $111.44 \text{ kJ/m}^3$  in melt-spun ribbons of Nd-Fe-B. At the same time, Sagawa et al<sup>[17-19]</sup> in Japan applied conventional powder metallurgy technology to ternary light-rare-earth-iron systems and obtained  $(BH)_{\max} \approx 287 \text{ kJ/m}^3$  for  $\text{Nd}_{15}\text{Fe}_{77}\text{B}_8$ . The excellent magnetic properties of these two systems are due to the highly anisotropic tetragonal  $R_2\text{Fe}_{14}\text{B}$  phase<sup>[20]</sup>. However, the Curie temperature of  $\text{Nd}_2\text{Fe}_{14}\text{B}$  is  $280\sim 310^\circ\text{C}$ , and the actual effective operating temperature is  $80\sim 200^\circ\text{C}$ <sup>[6,11,17,21]</sup>. Beyond this temperature,  $\text{Nd}_2\text{Fe}_{14}\text{B}$  magnets will be no longer appropriate for any dynamic applications. Future advanced power systems for aircraft, vehicles, and ships will require permanent magnetic materials that can be reliably operated at high temperatures up to  $450^\circ\text{C}$ <sup>[22,23]</sup>. The Co element can substitute for the entire composition range of Fe and has a significant effect on the magnetic Curie temperature<sup>[24-30]</sup>.

Received date: April 25, 2021

Foundation item: National Natural Science Foundation of China (51401130); Liaoning Provincial Natural Science Foundation of China (2019-MS-244); Liaoning Revitalization Talents Program (XLYC1907031); Liaoning BaiQianWan Talents Program (2020921082)

Corresponding author: You Junhua, Ph. D., Professor, School of Materials Science and Engineering, Shenyang University of Technology, Shenyang 110870, P. R. China, E-mail: youjunhua168@163.com

Copyright © 2022, Northwest Institute for Nonferrous Metal Research. Published by Science Press. All rights reserved.

Researchers have studied a large number of transition elements to substitute Fe to increase  $T_c$  and to improve thermal stability. Al, Si, and Ga alloying elements in Nd-Fe-B can also enhance thermal stability. However, the coercivity is decreased when Fe atoms are replaced by other elements. Thus, the addition of rare earth elements such as La, Ce, Pr, Sm, Gd, Dy or Tb to replace rare earth elements will cause Nd-Fe-B microstructure change which maintains the performance of coercivity<sup>[31-35]</sup>.

At present, there are many different preparation methods of Nd-Fe-B magnetic nanoparticles, which can be divided into physical methods and chemical methods. Conventional physical techniques mainly include melt quenching (MQ)<sup>[36,37]</sup>, hydrogenation disproportionation desorption recombination (HDDR)<sup>[38,39]</sup>, mechanical ball milling<sup>[40,41]</sup> and airflow grinding<sup>[42]</sup>. The physical preparation of magnetic powder is to crush a large alloy ingot into a certain size powder. Then, the ingot is simply crushed to 1~4 mm powder in an oxygen-free environment. Among these physical means, the HDDR method is the main technology of industrial production because it is easy to control and stable. However, there are many shortcomings in the physical methods, such as wide particle size distribution, poor control of microstructure, long process times and high cost. Thus, to avoid these disadvantages, researchers have studied the chemical preparation of nanoparticles  $Nd_2Fe_{14}B$  as the most promising alternative physical preparation method because it can better control the microstructure and grain size distribution. In addition, the use of metal salts as precursors significantly reduces the cost, such as chlorides, nitrates and acetylacetonates. The bottom-up chemical method allows the ions to be uniformly mixed, reducing the reaction temperature and producing uniformly distributed nanoparticles. Generally, there are several methods for synthesizing  $Nd_2Fe_{14}B$  nanoscale magnetic powder by chemical approaches, such as sol-gel<sup>[43-46]</sup>, microwave combustion<sup>[47-49]</sup>, thermal decomposition<sup>[50-54]</sup>, mechanochemical<sup>[55,56]</sup> and self-combustion method<sup>[57-59]</sup>.

In our previous study, we developed  $Nd_2Fe_{14}B$  nanoparticles and studied the formation mechanism by chemical method<sup>[53,54]</sup>. Here, several popular chemical methods for the synthesis of  $Nd_2Fe_{14}B$  nanoparticles are primarily introduced, and the technological flow and reaction mechanism of these methods are explained, which provides valuable insights for the future development of this research field.

## 1 Chemical Methods for the Synthesis of Nd-Fe-B Nanoparticles

The conventional physical process must go through high temperature homogenization, melting, casting, milling followed by annealing, and a series of process steps to obtain the final product. These multiple steps require large amounts of energy. Besides, these physical methods use high purity rare earth elements as their starting material. Usually, an excess amount of Nd is used to compensate for evaporation loss. Hence, the cost of production is increased. Besides, these

conventional techniques have difficulties in obtaining nanoparticles and controlling the microstructure. Therefore, chemical synthesis has attracted significant research interest due to better control of particle size.

The chemical synthesis of Nd-Fe-B can be divided into two important stages: Nd-Fe-B oxides and the reduction diffusion process. The oxides can be synthesized by dissolving metal ions in specific solutions, such as sol-gel, thermal decomposition method. However, in the mechanochemical method, metal oxides are directly used as raw materials, which are mixed with the reducing agent and then subjected to the chemical reaction by high-speed ball milling. In most cases, the mechanochemical reaction can be steady-state, resulting in a nano-sized product. The sample produces Nd-Fe-B nanoparticles after the reduction diffusion process. A vital advance in synthesizing Nd-Fe-B powder is the reduction diffusion technique. Ca has a high reduction potential of  $-2.87$  eV ( $Ca^{2+} \rightarrow Ca$ ). In the reduction diffusion process, Ca or  $CaH_2$  is used to reduce the metal oxides to obtain a magnetic powder. Later, the CaO byproduct needs to be removed. The magnetic properties of the final magnetic powder are closely related to the particle size and phase composition.

### 1.1 Sol-gel method

Sol-gel method is a method to synthesize hard magnetic nanoparticles based on solution synthesis and high temperature solid-state reduction diffusion<sup>[60]</sup>. In 2010, Deheri et al<sup>[61]</sup> fabricated  $Nd_2Fe_{14}B$  nanoparticles with an average particle size of  $\sim 50$  nm by the sol-gel method of chloride base metal salts. The coercivity and saturation magnetization of the washed powder were 310.44 and 736.56 kA/m, respectively. The synthetic route is shown in Fig. 1<sup>[61]</sup>. The thermal stable sol was prepared by adding a metal salt solution into a citric acid aqueous solution and a glycol aqueous solution. The mixed solution was magnetically stirred together to evaporate water, resulting in a viscous gel. After that, the dried gel was

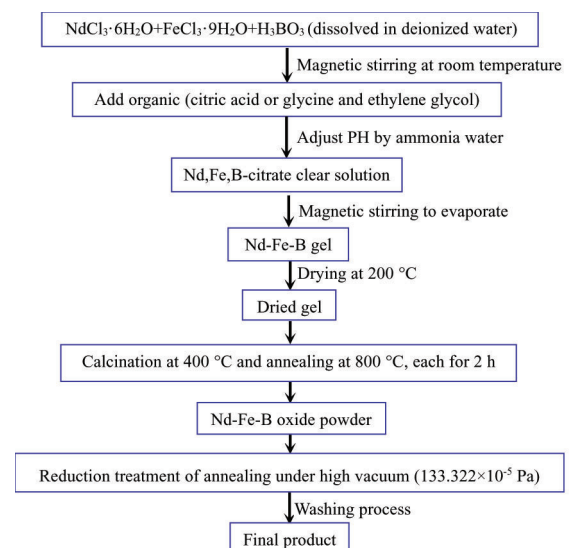


Fig.1 Flow chart of preparation of  $Nd_2Fe_{14}B$  magnetic powder via the sol-gel method<sup>[61]</sup>

annealed to prepare Nd<sub>2</sub>Fe<sub>14</sub>B oxide powder. Finally, the oxide powder was subjected to the reduction-diffusion process under vacuum ( $133.322 \times 10^{-5}$  Pa) to obtain the desired Nd<sub>2</sub>Fe<sub>14</sub>B phase. The team explained the reaction mechanism of this method in 2012<sup>[62]</sup>. It described that the metal oxide synthesized after annealing was composed of NdFeO<sub>3</sub> and M<sub>x</sub>O<sub>y</sub> (M=Nd, Fe, or B) phases. However, some articles evidence that oxide powders exist in NdBO<sub>3</sub> or Fe<sub>3</sub>BO<sub>5</sub> due to incomplete reaction temperature and time<sup>[63]</sup>. The reduction diffusion process of the Nd-Fe-B oxides (M<sub>x</sub>O<sub>y</sub>, M=Nd, Fe, B) by CaH<sub>2</sub> involved the following reactions<sup>[43,46,61]</sup>:



It is found that the Nd<sub>2</sub>Fe<sub>14</sub>B phase is formed by a direct combination of NdH<sub>2</sub>, Fe, and B by the following reactions:



The reaction takes place at 692 °C. To improve the hard magnetic phase crystallinity and to control particle size, it is very important to control the reaction temperature. In 2016, Rahimi et al<sup>[45]</sup> studied the effect of reduction temperature on Nd<sub>2</sub>Fe<sub>14</sub>B nanoparticles. The results showed that the average particle sizes of powders were about 84 nm at 750 °C. The temperature of reductive diffusion treatment changed the crystallinity of the sample which affected the magnetocrystalline anisotropy and particle size. The size of hard magnetic nanoparticles is closely related to the oxide powder, and the average size and coercivity of Nd-Fe-B oxide powder are also affected by the gel formed by different precursors. It is found that chloride base metal salts have better particle size and magnetic properties than nitrates<sup>[64]</sup>. Along with the size and crystallinity of the nanoparticles, chemical composition phase purity can also directly affect the magnetic property. Rahimi et al<sup>[44]</sup> reported that the coercivity of the nanoparticles was enhanced in Dy-substituted Nd-Fe-B nanoparticles in 2017. The maximum energy product, lowest-order uniaxial magnetocrystalline anisotropy constant, and Curie temperature had an upward trend as same as the coercivity.

The sol-gel method has some advantages compared to the physical method. In this method, the Nd-Fe-B magnetic powder with monodispersity and good control of the particle size can be obtained based on certain experimental conditions. At the same time, the microstructure and the homogeneity of the reaction products are controllable<sup>[65]</sup>. However, some shortcomings are inevitable for the sol-gel method, including long synthesis time of sol and gel, high energy consumption, and pollution from byproducts of reactions. Hence, it is limited in its efficiency.

## 1.2 Auto-combustion method

The novel auto-combustion method is based on the synthesis of a sol-gel which is also called sol-gel auto-combustion, through the combustion reaction of organic components and nitrate to obtain a homogeneous metal oxide powder<sup>[66]</sup>. The auto-combustion systems can be classified

according to the chemical composition of fuel, oxidizer and solvent. The fuels such as glycine, urea, citric acid and glycerol are used along with oxidizing agents like metal nitrates; water is used as a solvent in most works<sup>[67-69]</sup>.

In 2010, Bhame et al<sup>[59]</sup> reported the synthesis of magnetic Nd<sub>2</sub>Fe<sub>14</sub>B/α-Fe powders synthesized by a novel process of glycine nitrate auto-combustion followed by reduction diffusion. Glycine nitrate-based combustion of mixed metal nitrates is carried out to obtain homogeneously mixed oxide powders of FeNdO<sub>3</sub>. The composition of Nd-Fe-B oxides is similar to that of the sol-gel method, so the reduction-diffusion process is consistent. Moreover, by tuning the different compositions to synthesize higher energy products using the combustion method, the coercivity of 398 kA/m and energy product of 31.68 kJ/m<sup>3</sup> for magnetic powder were obtained. The Nd-Fe-B particle can be controlled in the size range from ~20 nm. The size of soft and hard nanocrystals plays an important role in promoting ferromagnetic exchange coupling between grains and the consequent enhancement of remanence and maximum energy density. The exchange coupling between the hard and soft phase is also related to the shape the material determine. The controllable Nd<sub>2</sub>Fe<sub>14</sub>B nanoparticle was almost spherical in shape with an average particle size of ~25 nm by the Jadhav team in 2012 (Fig.2)<sup>[58]</sup>. Furthermore, they found that the incorporation of excess neodymium would generate Nd and Fe soft magnetic phases and enhance exchange coupling with hard phase Nd<sub>2</sub>Fe<sub>14</sub>B in 2014<sup>[70]</sup>. The above fuel was glycine during combustion; citric acid was also successfully used as fuel to prepare Nd<sub>2</sub>Fe<sub>14</sub>B in 2015. Fig.3 showed the two routes of preparing oxides from citric acid and glycine as fuel. When citric acid is used as a fuel, it is necessary to add ammonia water, because the nitrate precursor reacts with ammonia to form NH<sub>4</sub>NO<sub>3</sub>, which decomposes and releases a large amount of heat to promote the combustion rate. The reaction is as follows<sup>[71]</sup>:



The glycine (fuel) -metal nitrate (oxidizer) system, the mixed solution of glycine, and metal nitrate were heated to form a viscous mass; continuous heating caused the viscous substance to catch fire and spontaneously burn to produce metal oxide mixture. The reaction mechanism is as follows, Me=Nd, Fe<sup>[66]</sup>:

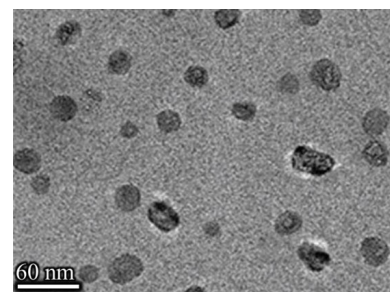


Fig.2 TEM image of Nd<sub>2</sub>Fe<sub>14</sub>B nanostructures by the auto-combustion method<sup>[58]</sup>

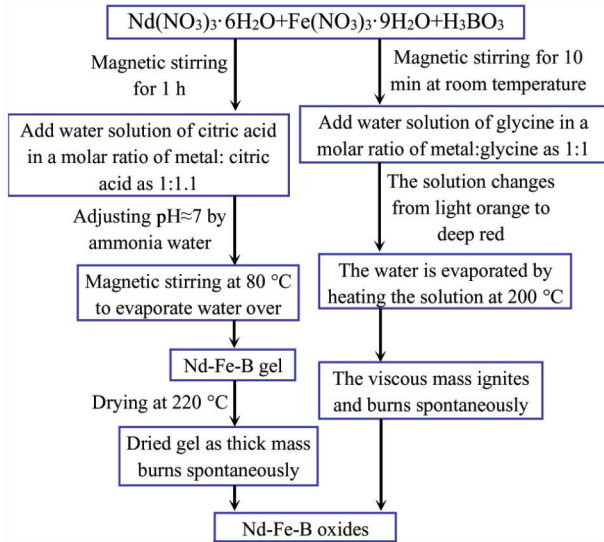
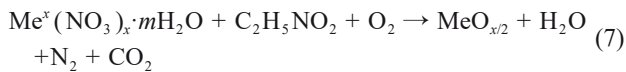


Fig.3 Flow chart of two routes of preparing oxides from citric acid and glycine as fuel<sup>[57,58,70]</sup>



In a word, the auto-combustion method saves energy consumption and shortens the time because the combustion reaction eliminates the need for high-temperature heating in the sol-gel preparation process.

### 1.3 Microwave-assisted combustion method

The microwave-assisted combustion method changes the heating method of the conventional tube furnace by the technology of microwave heating. The heating technology is that rapid relative movement occurs and electromagnetic energy is converted into heat energy for heating<sup>[72-74]</sup>. At present, there are few researches on synthesizing  $\text{Nd}_2\text{Fe}_{14}\text{B}$  by this heating technology. Except for the heating method, the microwave-assisted combustion synthesis process of hard magnetic particles is similar to the spontaneous combustion method. This microwave-assisted spontaneous combustion is caused by microwave irradiation of the solution which causes water to evaporate (Fig.4). The metal oxide after combustion is reduced and diffused under a vacuum environment. Finally, the magnetic powder is obtained after the byproduct removal. In 2014,  $\text{Nd}_2\text{Fe}_{14}\text{B}$  nanomagnetic particles were first successfully synthesized by Swaminathan et al<sup>[49]</sup> using the microwave combustion method. The coercivity of the resulting powders was about 636.9 kA/m, and the maximum magnetic energy product was 28.41 kJ/m<sup>3</sup>. It was reported that

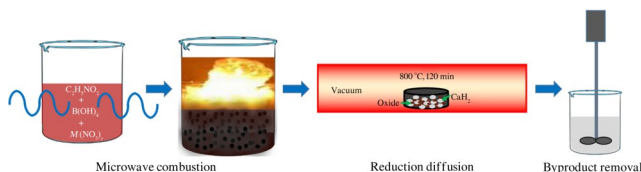
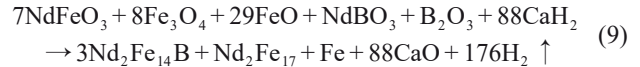
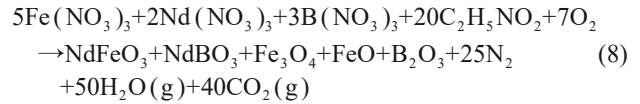


Fig.4 Schematic of the microwave process for the synthesis of Nd-Fe-B particles<sup>[75]</sup>

the reaction mechanism of the microwave combustion process is as follows:



In 2017, Parmar<sup>[43]</sup>, Tan<sup>[47]</sup> et al also successfully prepared  $\text{Nd}_2(\text{Fe}, \text{Co})_{14}\text{B}$  magnetic powder based on this mechanism in the same microwave chamber. The maximum energy product reached a value of 90.744 kJ/m<sup>3</sup>, which is the largest value among the reported values in chemical synthesis of  $\text{Nd}_2\text{Fe}_{14}\text{B}/\alpha\text{-Fe}$  nanoparticles. It showed that the microwave-assisted combustion method can better prepare metal oxides. The controllable microstructure and magnetic properties need to adjust the microwave power appropriately. Otherwise, higher microwave power will result in larger grain size. To enhance coercivity and improve thermal stability by increasing magnetocrystalline anisotropy, heavy rare earth Dy substitution on the magnetic properties was investigated in 2019<sup>[75]</sup>. The thermal stability of Nd-Fe-Co-Dy-B increased with the increase of Dy content. The coercive force increased first and then decreased after reaching the maximum value. Microwave heating technology can not only provide the reaction temperature for the synthesis of oxides but also reduce these oxides to prepare Nd-Fe-B hard magnetic powder in the same microwave chamber<sup>[48]</sup>. It can readily achieve one pot of synthesis of nanoscale magnetic powder.

The mechanism of microwave heating is the interaction between an electromagnetic wave and a dipolar molecule, so that the sample is heated evenly at the molecular level. In this method, processing needs less time and consumes less energy. Therefore, this is a promising method for obtaining a homogenous product. Nevertheless, microwaves easily couple with materials with heat generation inside the processed material. The inherent temperature gradient in microwave processing can lead to overheating of materials and form coarse particles, which will reduce the performance of materials.

### 1.4 Thermal decomposition method

The thermal decomposition reactions of organometallic compounds and metal surfactant complexes are performed in hot surfactant solutions in the presence of surfactants to synthesize nanoparticles of various materials<sup>[76]</sup>. Based on the synthesis of high-quality semiconductor nanocrystals and oxides in non-aqueous media by thermal decomposition<sup>[77-79]</sup>, different magnetic materials have also been developed by the way. Dispersed magnetic nanoparticles with small size can be obtained by thermal decomposition of organometallic compounds in high boiling point organic solvents containing stable surfactants<sup>[80,81]</sup>. The organometallic precursors include metal acetylacetonates [ $M(\text{acac})_n$ ], ( $M=\text{Nd}, \text{Fe}, \text{Mn}, \text{Co}, \text{Ni}, \text{Cr}; n=2$  or  $3$ , acac=acetylacetonate), metal cupferronates [ $Mx\text{Cupx}$ ] ( $M$ =metal ion; Cup=N-nitrosophenylhydroxylamine,  $\text{C}_6\text{H}_5\text{N}(\text{NO})\text{O}$ -)<sup>[82]</sup> or carbonyls<sup>[83]</sup>. Fatty acids<sup>[84]</sup>, oleic acids<sup>[85]</sup>, and hexadecylamine<sup>[86]</sup> are often used as surfactants.

The metal acetylacetonates as precursors successfully synthesized  $\text{Nd}_2\text{Fe}_{14}\text{B}/\alpha\text{-Fe}$  nanoparticles by chemical thermal decomposition method in 2013 by Yu et al.<sup>[51]</sup>. The next year, they showed that high exchange coupled  $\text{Nd}_2\text{Fe}_{14}\text{B}/\text{Fe}_3\text{B}$  composites were synthesized with a large coercivity of  $\sim 875.6$  kA/m, and  $M_r/M_{3T}=0.59$ <sup>[50]</sup>. In 2018, our group have successfully synthesized  $\text{Nd}_2\text{Fe}_{14}\text{B}$  nanoparticles and presented the reaction mechanism by the thermal decomposition approach<sup>[53]</sup>. Table 1 shows the reaction mechanism of the prepared  $\text{Nd}_2\text{Fe}_{14}\text{B}$ . The acetylacetonate salt and  $(\text{C}_2\text{H}_5)_3\text{NBH}_3$  are decomposed into  $\text{Nd}^{3+}$ ,  $\text{Fe}^{2+}$ ,  $\text{Fe}^{3+}$ , and  $\text{BH}_3^-$  at 260~350 °C to the form a simple metal nucleus (reaction 1~3). The metal nucleus Nd combines with the unreduced metal oxides  $\text{Fe}_3\text{O}_4$  to form  $\text{NdFeO}_3$  under a constant flow of Ar+5%  $\text{H}_2$  gas (reaction in Eq.(4~5)). Moreover, some neodymium may react with  $\text{HBO}_2$  after hydrolysis to form  $\text{NdBO}_3$  (reaction in Eq. (6)). Eventually, the metal oxides ( $\text{NdFeO}_3$ ,  $\text{NdBO}_3$ , Fe) are reduced with  $\text{CaH}_2$  to synthesize the  $\text{Nd}_2\text{Fe}_{14}\text{B}$  phase (reaction in Eq. (7~9)). In this method, to obtain uniformly distributed nanoparticles and more hard magnetic phases, we investigated the effects of B addition amount and reduction diffusion time on magnetic powder<sup>[54]</sup>. The results showed that the  $\text{H}_5\text{Nd}_2$  phase was produced since the boron content was low, and the particles would agglomerate when there was too much boron. Excellent average grain size and magnetic properties of  $\text{Nd}_2\text{Fe}_{14}\text{B}$ , can be obtained by adjusting the appropriate reduction diffusion time, as shown in Fig. 5<sup>[87]</sup>. When the reduction and diffusion process is maintained for 180 min, the striped crystal plane of Nd can be clearly seen in the HRTEM image. The crystal plane spacing is 0.440 nm (the crystal plane (200)). The Nd-rich phase boundary appears at the hard magnetic phase boundary which will hinder the movement of the hard magnetic phase magnetic chip at the phase boundary to increase the coercivity. The average grain size of this region is measured to be 40.60 nm. It will affect the exchange coupling between the grains and enhance the magnetic energy product.

In general, the magnetic nanoparticles have good size control, narrow size distribution and good magnetic properties by thermal decomposition method, because the surfactant in an organic solvent can inhibit the growth of the particles at a certain temperature and time. However, due to the addition of

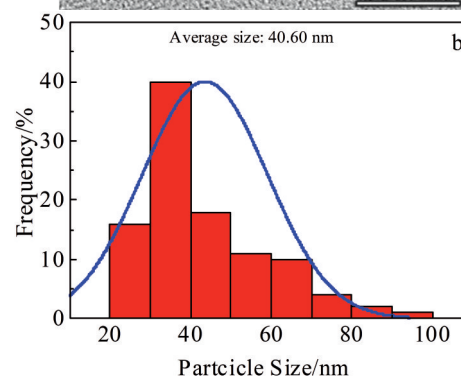
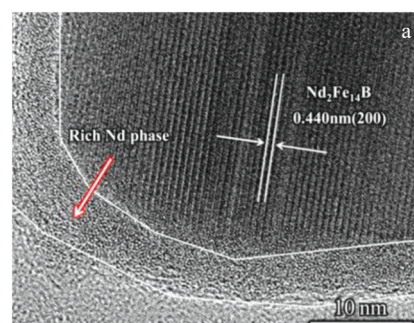


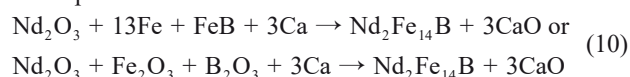
Fig.5 HRTEM image (a) and average particle size distribution (b) of nanocrystalline Nd-Fe-B powders obtained by holding for 180 min<sup>[87]</sup>

organic matter, a large amount of preliminary cleaning is required. Otherwise, the reduction of oxides and the diffusion process of elements will be affected.

### 1.5 Mechanochemical method

The technique was originally developed in the mid-1960s to produce oxide-dispersion strengthened superalloys and to synthesize various alloy phases, including solid solutions, quasicrystalline, crystalline phases and amorphous phases<sup>[88]</sup>. In recent years, the mechanochemical technique has been applied to the synthesis of various hard magnetic particles, including  $\text{Sm}_2\text{Co}_{17}$ ,  $\text{Nd}_2\text{Fe}_{14}\text{B}$ ,  $\text{LaCo}_5$ , etc.<sup>[88-90]</sup>.

In 2016, Pal<sup>[91]</sup> synthesized  $\text{Nd}_2\text{Fe}_{14}\text{B}$  for the first time through the mechanochemical process with the coercivity of about 955.2 kA/m and the grain thickness of 50~70 nm. The reaction processes involved are as follows<sup>[42,91]</sup>:



The mechanochemical process for the synthesis of Nd-Dy-Fe-Co-B particles is shown in Fig. 6<sup>[92]</sup>. In mechanochemical processing, low-cost metal oxides are used as raw materials. The metal oxide is well mixed with the reducing agent calcium. In the process of mechanical high-speed ball grinding, metal oxides are partially reduced and broken. The desired tetragonal crystal structure of the Nd-Fe-B nanoparticles is observed after annealing. The addition of Co atoms replaced some Fe atoms, which increased the Fe-Fe atomic spacing and the exchange between 3d-3d, and the magnetic properties were maintained at high temperatures<sup>[93,94]</sup>. Part of the existing Co atoms combined with Nd and Fe atoms to

Table 1 Thermal decomposition reaction process<sup>[52-54]</sup>

No.	Reaction
1	$2\text{BH}_3 + 4\text{H}_2\text{O} = 2\text{BO}_2 + 7\text{H}_2 \uparrow$
2	$n\text{BH}_3 + 7M^{n+} + 7n\text{OH}^- = n\text{BO}_2 + 7M + 5n\text{H}_2\text{O}$
3	$2\text{H}^+ + 2\text{BO}_2^- = 2\text{HBO}_2$
4	$\text{Fe}_3\text{O}_4 + \text{H}_2 \triangleq \text{Fe} + \text{H}_2\text{O}$
5	$4\text{Nd} + 3\text{Fe}_3\text{O}_4 = 4\text{NdFeO}_3 + 5\text{Fe}$
6	$2\text{Nd} + 2\text{H}_2\text{O} + 2\text{HBO}_2 = 2\text{NdBO}_3 + 3\text{H}_2 \uparrow$
7	$4\text{NdFeO}_3 + 12\text{CaH}_2 = 2\text{H}_5\text{Nd}_2 + 4\text{Fe} + 12\text{CaO} + 7\text{H}_2 \uparrow$
8	$4\text{NdBO}_3 + 12\text{CaH}_2 = 2\text{H}_5\text{Nd}_2 + 4\text{B} + 12\text{CaO} + 7\text{H}_2 \uparrow$
9	$2\text{H}_5\text{Nd}_2 + 28\text{Fe} + 2\text{B} = 2\text{Nd}_2\text{Fe}_{14}\text{B} + 5\text{H}_2 \uparrow$

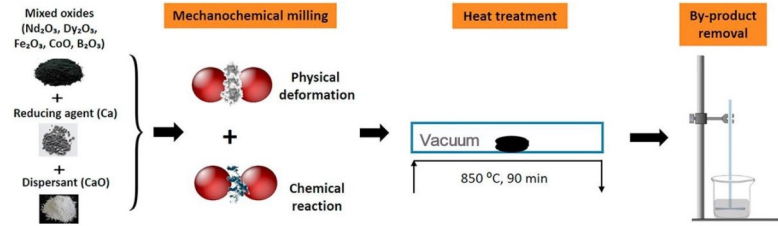


Fig.6 Schematic of the mechanochemical process for the synthesis of Nd-Dy-Fe-Co-B particles<sup>[92]</sup>

form a soft magnetic phase at the grain boundary. This soft magnetic phase reduced the coercivity of the material. Therefore, the addition of rare earth elements Dy to replace rare earth elements will cause Nd-Fe-B microstructure changes that maintain the performance of coercivity<sup>[31-35]</sup>. In a word, partial substitution of the Nd element affects the formation of new phases at the Nd-Fe-B grain boundary, which is conducive to the isolation of adjacent hard magnetic grains, and then increases coercivity<sup>[64,95]</sup>. It has been reported that substitution of a small amount of Fe by Cr in  $\text{Nd}_2(\text{Fe}_{11.25}\text{Co}_2\text{Cr}_{0.75})\text{B}$  is also helpful to increasing the coercivity<sup>[96]</sup>. There are two reasons for substituting small amounts of Cr for Fe: one is to increase coercivity and the other is to improve corrosion resistance.

The mechanochemical method is a low-cost and scalable process to produce high coercivity Nd-Fe-B magnetic nanoparticles because the raw materials are cheap and the preparation rate is simple. More importantly, this technology has also been applied to the recovery of different rare earth elements in the Nd-Fe-B magnet, which is of great significance for the future research of recycling<sup>[97,98]</sup>.

## 2 Microstructure and Magnetic Properties of Nd-Fe-B Nanoparticles Prepared by Different Chemical Methods

In order to study the relationship between microstructure and magnetic properties of Nd-Fe-B nanoparticles prepared by different chemical methods, the SEM micrographs of the powder are shown in Fig. 7. Fig. 7a shows the microstructure of Nd-Fe-B prepared by sol-gel method. It can be seen that the bulk and flake grains are clustered together and the grain size and direction are not uniform, which might lead to the formation of reverse magnetic chips, reducing the residual magnetization of the magnet. When using automatic combustion preparation, it can be observed from Fig. 7b that the adhesion phenomenon occurs between grains, which might be due to insufficient combustion of organic matter in the combustion process, or the phenomenon of grain fusion due to too high combustion temperature. Similarly, combined with the SEM image in Fig. 7c, it can be seen that in the microwave-assisted combustion process, the aggregation of particles is more serious and the grain boundaries are blurred. There are a large number of voids in this area, which decrease the magnetic energy product of the magnet. Therefore, it is

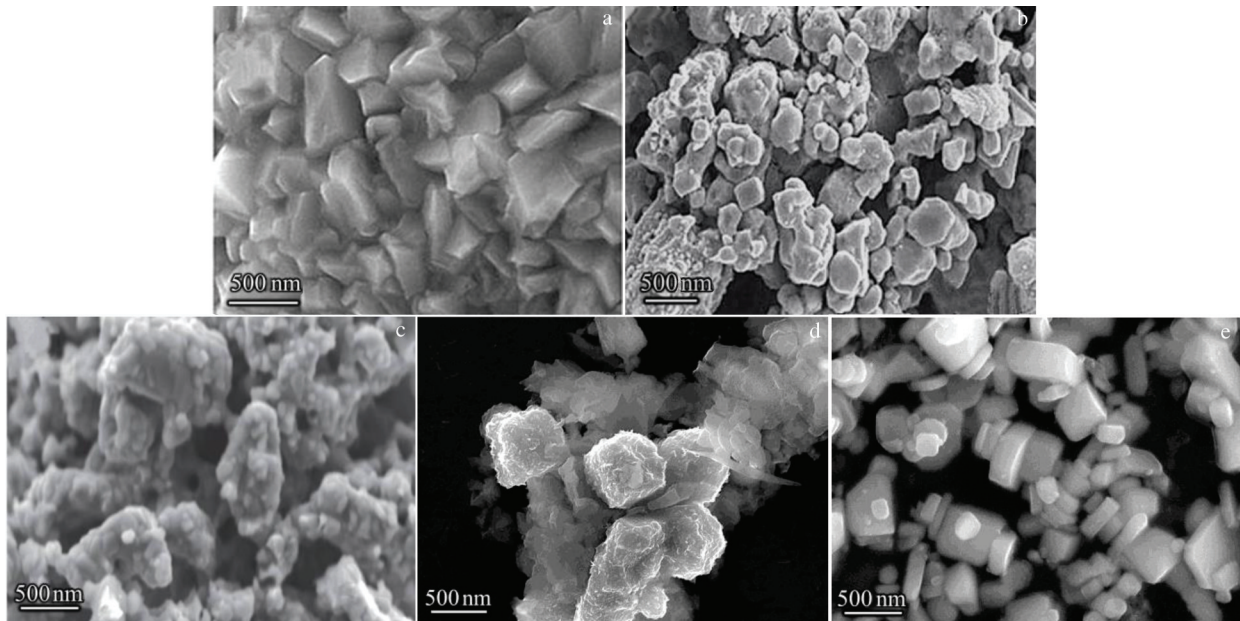


Fig.7 SEM images of  $\text{Nd}_2\text{Fe}_{14}\text{B}$  nanostructures by sol-gel<sup>[45]</sup> (a), auto-combustion<sup>[57]</sup> (b), microwave-assisted combustion<sup>[59]</sup> (c), thermal decomposition<sup>[53]</sup> (d), and mechanochemical method<sup>[35]</sup> (e)

**Table 2** Summary of preparation of Nd<sub>2</sub>Fe<sub>14</sub>B magnetic nanoparticles by the chemical method after wash

Method	Phase	$H_c/kA \cdot m^{-1}$	$(BH)_{max}/kJ \cdot m^{-3}$	Average grain size/nm	Ref.
Sol-gel	Nd <sub>2</sub> Fe <sub>14</sub> B	74.7	159.2	60	[44]
Sol-gel	Nd <sub>2</sub> Fe <sub>14</sub> B/Nd <sub>2</sub> Fe <sub>17</sub> $\alpha$ -Fe	264.3	127.4	30~65	[99]
Auto-combustion	Nd <sub>2</sub> Fe <sub>14</sub> B	~261.3	~43	100~150	[57]
Microwave	Nd <sub>2</sub> Fe <sub>14</sub> B /Nd <sub>2</sub> Fe <sub>17</sub> / $\alpha$ -Fe	262.7	28.4	~80	[49]
Microwave	Nd <sub>2</sub> Fe <sub>14</sub> B / $\alpha$ -Fe	716.4	41.4	62	[43]
Thermal decomposition	Nd <sub>2</sub> Fe <sub>14</sub> B / $\alpha$ -Fe	460.9	20	31	[53]
Thermal decomposition	Nd <sub>2</sub> Fe <sub>14</sub> B /Fe <sub>3</sub> B	~884	~199	10~25	[50]
Mechanochemical	Nd <sub>2</sub> Fe <sub>14</sub> B / $\alpha$ -Fe	262.7	-	100	[34]
Mechanochemical	Nd <sub>2</sub> Fe <sub>14</sub> B	366.2	-	60~140	[35]

necessary to control the heating power to improve the stability of the process during the microwave heating process. Fig. 7d shows the microstructure of the magnetic powder synthesized by thermal decomposition method. The crystal grains in this area are uniformly distributed in layers. The original dispersed particles formed blocks through the process of reduction and diffusion, and the lamellar structure grows further. The surface of the cube is wrapped in new phases, and the continuous grain boundary begins to fuse together at high temperatures. Based on mechanochemical method, some intact tetragonal grains and partially damaged particles can be seen in Fig. 7e. At the same time, in the scanning area, it can be observed that there are unevenly distributed small particles around the large particles. These grain structures are deformed and dislocated during the mechanical ball milling process, which changes the anisotropy of the Nd-Fe-B crystal and the anisotropy of the Nd-Fe-B tetragonal crystal. It reduces the magnetic energy product and uniform distribution of magnetic powder.

Table 2 summarizes the phase composition, magnetic properties, and average grain size of Nd<sub>2</sub>Fe<sub>14</sub>B powders synthesized by different chemical methods from the literature of recent years. It shows that the maximum coercivity of 460.9 kA/m is synthesized by thermal decomposition. The high coercivity is due to the fact that the average crystal grain size (~20 nm) is close to the width of the domain wall to form a single domain body. In addition, in the case of a single domain body, because the adjacent atoms of the hard magnetic and soft magnetic phases are in direct contact, the magnetic moment of the hard magnetic grain atoms is along the direction of magnetization, the anisotropy of the soft magnetic is low, and the hard magnetic phase forces the atomic magnetic moment of the soft magnetic grain to be consistent with that of the hard magnetic phase, so that the soft magnetic grain is transformed into the hard magnetic grain. Therefore, the coercivity of the magnetic powder is improved. The excellent maximum energy product  $(BH)_{max}=159.2$  kJ/m<sup>3</sup> was synthesized by the sol-gel method because of nanocomposite magnets consisting of a mixture of exchange coupled hard and soft phases and narrow grain size distribution. Considering the cost of synthesis, the mechanochemical method only needs metal oxide as raw material, two-step synthesis of hard

magnetic phase through high-energy ball milling and reduction diffusion process. However, according to the microstructure image in Fig. 7 and the results in Table 2, it is revealed that the size of the powder synthesized by mechanochemical method is about 100 nm, and the large average grain size powder will affect the magnetic property inconsistency of the product. In terms of energy consumption and time, microwave-assisted combustion and auto-combustion make full use of spontaneous combustion reaction to reduce external heating energy, while the synthesis time is shorter than other methods. It should be considered that control of combustion temperature and rate is necessary to prevent the occurrence of wide grain size distribution and soft magnetic phase.

### 3 Conclusions and Perspectives

This study introduces the process flow, microstructure and magnetic properties of Nd-Fe-B prepared by chemical methods in recent years. The synthesis of Nd-Fe-B magnetic powder is important for high performance permanent magnet and production cost. Thus, thermal decomposition method and mechanochemistry method are more in line with the actual product production needs in these chemical methods.

Research on nanoparticles in hard magnetic materials is expected to optimize the phase composition and grain size distribution, which can increase the exchange coupling effect of hard magnetic phase and soft magnetic phase, and improve the coercive force and magnetic energy product of the magnet. Also, for future applications, the mechanical properties of nanoparticles synthesized magnets are expected to be better than those of very brittle classic sintered magnets. However, the synthesis of high-quality Nd-Fe-B hard magnetic nanoparticles is practically still a challenge. It is necessary to synthesize Nd-Fe-B nanoparticles by the green chemical method. Besides, extensive studies are needed to maintain the long-term stability and purity of powder without agglomeration or precipitation. For Nd<sub>2</sub>Fe<sub>14</sub>B magnetic powder sensitive to air or water, we should develop effective strategies to improve its chemical stability, such as adding metal Co, Dy, Cr. We expect that Nd-Fe-B hard magnetic

nanoparticles will occupy more important positions in the functional material field.

## References

- 1 Zhang J, Song J Z, Zhang Y et al. *IEEE Transactions on Magnetics*[J], 2011, 47(10): 2792
- 2 Rong C B, Zhang H W, Chen R J et al. *Journal of Physics D-Applied Physics*[J], 2006, 39(3): 437
- 3 Poudyal N, Liu J P. *Journal of Physics D-Applied Physics*[J], 2013, 46(4): 23
- 4 Gutfleisch O, Willard M A, Bruck E et al. *Advanced Materials* [J], 2011, 23(7): 821
- 5 Liu X Y, Li Y P, Hu L X. *Rare Metal Materials and Engineering* [J], 2012, 41(10): 1875 (in Chinese)
- 6 Sugimoto S. *Journal of Physics D-Applied Physics*[J], 2011, 44(6): 110
- 7 Li G D. *Rare Metal Materials and Engineering*[J], 2005, 34(5): 673
- 8 Hadjipanayis G C. *Journal of Magnetism and Magnetic Materials*[J], 1999, 200(1-3): 373
- 9 Li Z B, Liu X C, Pan J et al. *Rare Metal Materials and Engineering* [J], 2010, 39(10): 1868 (in Chinese)
- 10 Clark A. *Applied Physics Letters*[J], 1974, 23: 642
- 11 Herbst J F. *Reviews of Modern Physics*[J], 1991, 63(4): 819
- 12 Koon N C, Das B N. *Journal of Applied Physics*[J], 1984, 55(6): 2063
- 13 Hadjipanayis G C, Hazelton R C, Lawless K R. *Journal of Applied Physics*[J], 1984, 55(6): 2073
- 14 Croat J J, Herbst J F, Lee R W et al. *Journal of Applied Physics* [J], 1984, 55(6): 2078
- 15 Becker J J. *Journal of Applied Physics*[J], 1984, 55(6): 2067
- 16 Croat J, Herbst J, Lee R et al. *Applied Physics Letters*[J], 1984, 44: 148
- 17 Sagawa M, Fujimura S, Togawa N et al. *Journal of Applied Physics*[J], 1984, 55(6): 2083
- 18 Hirosawa S, Matsuura Y, Yamamoto H et al. *Journal of Applied Physics*[J], 1986, 59(3): 873
- 19 Hirosawa S, Matsuura Y, Yamamoto H et al. *Japanese Journal of Applied Physics Part 2-Letters*[J], 1985, 24(10): 803
- 20 Herbst J, Croat J, Pinkerton F et al. *Physical Review B*[J], 1984, 29(7): 4176
- 21 Betancourt I, Davies H A. *Materials Science and Technology*[J], 2010, 26(1): 5
- 22 Zhu Z Q, Howe D. *IEEE Proceedings-Electric Power Applications*[J], 2001, 148(4): 299
- 23 Coey J M D. *Scripta Materialia*[J], 2012, 67(6): 524
- 24 Wei G, Hadjipanayis G C, Krause R F. *Journal of Applied Physics*[J], 1994, 75(10): 6649
- 25 Kim A S, Camp F E. *Journal of Applied Physics*[J], 1996, 79(8): 5035
- 26 Liu J F, Davies H A. *Journal of Magnetism and Magnetic Materials*[J], 1996, 157: 29
- 27 Chang W C, Wu S H, Ma B M et al. *Journal of Applied Physics* [J], 1998, 83(4): 2147
- 28 Mottram R S, Williams A J, Harris I R. *Journal of Magnetism and Magnetic Materials*[J], 2000, 217(1-3): 27
- 29 Neu V, Schultz L. *Journal of Applied Physics*[J], 2001, 90(3): 1540
- 30 Bai G, Gao R W, Sun Y et al. *Journal of Magnetism and Magnetic Materials*[J], 2007, 308(1): 20
- 31 Yan C, Guo S, Chen R et al. *IEEE Transactions on Magnetics*[J], 2014, 50(10): 1
- 32 Pandian S, Chandrasekaran V, Markandeyulu G et al. *Journal of Alloys and Compounds*[J], 2004, 364(1-2): 295
- 33 Burzo E. *Reports on Progress in Physics*[J], 1998, 61(9): 1099
- 34 Koylu-Alkan O, Barandiaran J M, Salazar D et al. *AIP Advances* [J], 2016, 6(5): 56 027
- 35 Gabay A M, Hu X C, Hadjipanayis G C. *Journal of Alloys and Compounds*[J], 2013, 574: 472
- 36 Brown D N, Chen Z, Guschl P et al. *Journal of Magnetism and Magnetic Materials*[J], 2006, 303(2): 371
- 37 Lin X, Luo Y, Peng H J et al. *Journal of Magnetism and Magnetic Materials*[J], 2019, 490: 165 454
- 38 Kim T H, Kang M C, Lee J G et al. *Journal of Alloys and Compounds*[J], 2018, 732: 32
- 39 Zhang F, Liu Y, Li J et al. *Journal of Alloys and Compounds*[J], 2018, 750: 401
- 40 An X, Jin K, Abbas N et al. *Journal of Magnetism and Magnetic Materials*[J], 2017, 442: 279
- 41 An X, Jin K, Wang F et al. *Materials Research Express*[J], 2017, 4(2): 25 033
- 42 Liu X, Hu L, Mei Y. *International Journal of Hydrogen Energy* [J], 2013, 38(31): 13 694
- 43 Parmar H, Xiao T, Chaudhary V et al. *Nanoscale*[J], 2017, 9(37): 13 956
- 44 Rahimi H, Ghasemi A, Mozaffarinia R et al. *Journal of Magnetism and Magnetic Materials*[J], 2017, 429: 182
- 45 Rahimi H, Ghasemi A, Mozaffarinia R et al. *Journal of Superconductivity and Novel Magnetism*[J], 2016, 29(8): 2041
- 46 Zhang J S, Wu W, Meng F S et al. *Modern Physics Letters B*[J], 2018, 32(34-36): 1 840 070
- 47 Tan X, Parmar H, Zhong Y et al. *IEEE Magnetics Letters*[J], 2017, 8: 1
- 48 Tan X, Parmar H, Chaudhary V et al. *New Journal of Chemistry* [J], 2018, 42(23): 19 214
- 49 Swaminathan V, Deheri P K, Bhame S D et al. *Nanoscale*[J], 2013, 5(7): 2718
- 50 Yu L Q, Zhang Y P, Yang Z et al. *Nanoscale*[J], 2016, 8(26): 12 879
- 51 Yu L Q, Yang C, Hou Y L. *Nanoscale*[J], 2014, 6(18): 10 638
- 52 Jeong J H, Ma H X, Kim D et al. *New Journal of Chemistry*[J], 2016, 40(12): 10 181

- 53 Guo Y Z, Zhao D, You J H et al. *RSC Advances*[J], 2018, 8(68): 38 850
- 54 Guo Y Z, You J H, Pei W L et al. *Journal of Alloys and Compounds*[J], 2019, 777: 850
- 55 Zhong Y, Chaudhary V, Tan X et al. *Journal of Alloys and Compounds*[J], 2018, 747: 755
- 56 Zhong Y, Chaudhary V, Tan X et al. *Nanoscale*[J], 2017, 9(47): 18 651
- 57 Ma H X, Kim C W, Kim D S et al. *Nanoscale*[J], 2015, 7(17): 8016
- 58 Jadhav A P, Hussain A, Lee J H et al. *New Journal of Chemistry* [J], 2012, 36(11): 2405
- 59 Bhame S D, Swaminathan V, Deheri P K et al. *Advanced Science Letters*[J], 2010, 3(2): 174
- 60 Sheridan R S, Sillitoe R, Zakotnik M et al. *Journal of Magnetism and Magnetic Materials*[J], 2012, 324(1): 63
- 61 Deheri P K, Swaminathan V, Bhame S D et al. *Chemistry of Materials*[J], 2010, 22(24): 6509
- 62 Deheri P K, Shukla S, Ramanujan R V. *Journal of Solid State Chemistry*[J], 2012, 186: 224
- 63 Deheri P K, Swaminathan V, Bhame S D et al. *Chemistry of Materials*[J], 2010, 22(24): 6509
- 64 Chen W, Gao R W, Zhu M G et al. *Journal of Magnetism and Magnetic Materials*[J], 2003, 261(1-2): 222
- 65 Hench L L, West J K. *Chemical Reviews*[J], 1990, 90(1): 33
- 66 Varma A, Mukasyan A S, Rogachev A S et al. *Chemical Reviews* [J], 2016, 116(23): 14 493
- 67 Huang J, Zhuang H, Li W. *Journal of Magnetism and Magnetic Materials*[J], 2003, 256(1): 390
- 68 Suresh K, Patil K C. *Journal of Solid State Chemistry*[J], 1992, 99(1): 12
- 69 Sileo E E, Rotelo R, Jacobo S E. *Physica B-Condensed Matter* [J], 2002, 320(1-4): 257
- 70 Jadhav A P, Ma H, Kim D S et al. *Bulletin of the Korean Chemical Society*[J], 2014, 35(3): 886
- 71 Liu J, Zeng Y, Guo C et al. *Journal of the European Ceramic Society*[J], 2010, 30(4): 993
- 72 Mishra R R, Sharma A K. *Composites Part A-Applied Science and Manufacturing*[J], 2016, 81: 78
- 73 Buchelnikov V D, Louzguine-Luzgin D V, Anzulevich A P et al. *Physica B-Condensed Matter*[J], 2008, 403(21-22): 4053
- 74 Sun J, Wang W H, Yue Q Y. *Materials*[J], 2016, 9(4): 231
- 75 Tan X, Parmar H, Zhong Y et al. *Journal of Magnetism and Magnetic Materials*[J], 2019, 471: 278
- 76 Park J, Joo J, Kwon S G et al. *Angewandte Chemie-International Edition*[J], 2007, 46(25): 4630
- 77 Murray C B, Norris D J, Bawendi M G. *Journal of the American Chemical Society*[J], 1993, 115(19): 8706
- 78 Peng X, Wickham J, Alivisatos A P. *Journal of the American Chemical Society*[J], 1998, 120(21): 5343
- 79 O'Brien S, Brus L, Murray C B. *Journal of the American Chemical Society*[J], 2001, 123(48): 12 085
- 80 Redl F X, Black C T, Papaefthymiou G C et al. *Journal of the American Chemical Society*[J], 2004, 126(44): 14 583
- 81 Sun S, Zeng H, Robinson D B et al. *Journal of the American Chemical Society*[J], 2004, 126(1): 273
- 82 Rockenberger J, Scher E C, Alivisatos A P. *Journal of the American Chemical Society*[J], 1999, 121(49): 11 595
- 83 Farrell D, Majetich S A, Wilcoxon J P. *The Journal of Physical Chemistry B*[J], 2003, 107(40): 11 022
- 84 Jana N R, Chen Y, Peng X. *Chemistry of Materials*[J], 2004, 16(20): 3931
- 85 Samia A C S, Hyzer K, Schlueter J A et al. *Journal of the American Chemical Society*[J], 2005, 127(12): 4126
- 86 Li Y, Afzaal M, O'Brien P. *Journal of Materials Chemistry*[J], 2006, 16(22): 2175
- 87 Pei W L, Zhang X H, Meng Q Y et al. *Materials Research Express*[J], 2019, 6(10): 9
- 88 Suryanarayana C, Nasser, Al-Aqeeli N. *Progress in Materials Science*[J], 2013, 58(4): 383
- 89 Gabay A M, Hu X C, Hadjipanayis G C. *Journal of Magnetism and Magnetic Materials*[J], 2014, 368: 75
- 90 Li W F, Gabay A M, Hu X C et al. *Journal of Physical Chemistry C*[J], 2013, 117(20): 10 291
- 91 Pal A, Gabay A, Hadjipanayis G C. *Journal of Alloys and Compounds*[J], 2012, 543: 31
- 92 Zhong Y, Chaudhary V, Tan X et al. *Journal of Magnetism and Magnetic Materials*[J], 2019, 475: 554
- 93 Ma B M, Narasimhan K. *IEEE Transactions on Magnetics*[J], 1986, 22(5): 916
- 94 Buschow K H J, Demooij D B, Sinnema S et al. *Journal of Magnetism and Magnetic Materials*[J], 1985, 51(1-3): 211
- 95 Fu W, Guo S, Lin C et al. *IEEE Transactions on Magnetics*[J], 2013, 49(7): 3258
- 96 Chaudhary V, Zhong Y, Parmar H et al. *Chemphyschem*[J], 2018, 19(18): 2370
- 97 Van Loy S, Onal M A R, Binnemans K et al. *Hydrometallurgy* [J], 2020, 191: 105 154
- 98 Sasai R, Shimamura N, Fujimura T. *ACS Sustainable Chemistry & Engineering*[J], 2020, 8(3): 1507
- 99 Rahimi H, Ghasemi A, Mozaffarinia R et al. *Journal of Magnetism and Magnetic Materials*[J], 2017, 444: 111

## 化学法合成 Nd-Fe-B 磁性纳米粒子的评述—微结构与磁性能

孟庆宇, 尤俊华, 周继凤, 刘子宇  
(沈阳工业大学 材料科学与工程学院, 辽宁 沈阳 110870)

**摘要:** 高性能钕铁硼磁体广泛应用于各个领域。当 Nd-Fe-B 磁粉的晶粒尺寸接近单畴临界尺寸时, 其矫顽力最大。化学法制备 Nd-Fe-B 磁粉可以很好地控制磁粉的微观结构和晶粒尺寸。同时, 金属盐作为前驱体和简单的工艺流程可以降低成本和能源损耗。介绍了几种化学法制备 Nd-Fe-B 磁粉, 分别为溶胶凝胶法、自燃烧法、微波辅助燃烧法、热分解法和机械化学法。研究了这些化学法的制备工艺和反应机理。最后, 对不同化学方法合成的 Nd-Fe-B 磁粉的显微组织进行了对比分析, 阐述了显微组织与磁性能之间的联系, 展望了磁性材料未来的发展趋势。

**关键词:** 钕铁硼; 磁性纳米粒子; 化学法合成; 居里温度

---

作者简介: 孟庆宇, 男, 1996年生, 硕士, 沈阳工业大学材料科学与工程学院, 辽宁 沈阳 110870, E-mail: 1621950169@qq.com